Rationalizing Ring-Size Selectivity in Intramolecular Pd-Catalyzed Allylations of Resonance-Stabilized Carbanions

Per-Ola Norrby,*[,§] Mary M. Mader,[‡] Maxime Vitale,[†] Guillaume Prestat,[†] and Giovanni Poli*[,†]

Department of Chemistry, Building 201, Technical University of Denmark, Kemitorvet, DK-2800 Kgs. Lyngby, Denmark, Eli Lilly and Company, Lilly Corporate Center, Drop Code 1523, Indianapolis, Indiana, 46285, and the Laboratoire de Chimie Organique, UMR 7611 CNRS, Université Pierre et Marie Curie, Tour 44-45, 4, Place Jussieu, Boîte 183, F-75252, Paris, Cedex 05, France

Received January 28, 2003

Computational methods were applied to the Pd-catalyzed intramolecular allylations of resonance-stabilized carbanions obtained from amide and ketone substrates, with the aim of rationalizing the endo vs exo selectivity in the cyclizations. In addition, ester substrates were prepared and subjected to the Pd-catalyzed cyclization conditions, and were found to form lactones via exo attack. DFT calculations with the BP86/LACVP*+ level of theory with a CH_2Cl_2 solvation correction reproduce the relative transition state energies. The preference for exo-cyclization of the nitrogen-containing starting material appears to result from the preference for near-planarity of the amide N. Both the oxygen and nitrogen tethers are too short to allow efficient endo cyclization, whereas the carbon tether is long enough to allow favorable endo cyclization. The carbon tether also disfavors the exo cyclization transition states slightly from eclipsing interaction, leading to almost isoenergetic exo and endo transition states, and thus accounting for the experimentally observed mixture of five- and seven-membered-ring products.

Introduction

A few years ago some of us reported a novel Pd-catalyzed route to 3,4-disubstituted pyrrolidones.[1] Such a cyclization process was based on the interaction between a resonance-stabilized carbanion and an allylic acetate function, tethered by a nitrogen atom (Scheme 1). Careful analysis of the reaction products in all the cases studied revealed that the reaction is completely regio- and stereoselective. In fact, the trans 3,4-disubstituted pyrrolidone was always obtained as the only isomer.

Although the stereoselectivity of this transformation appears to be rationalizable on the basis of a fast base-catalyzed product equilibration at the enolizable position, a straightforward understanding of the regiochemical outcome seemed more intriguing. Indeed, although the pyrrolidone ring was the expected cyclization product, the total absence of azepinone, according to a potential competitive 7-endo process, could not be anticipated from the outset. The above consideration becomes especially important in view of the results reported by Tsuji et al.,[2] and later confirmed by the Pfalz group[3] in the context of the analogous cyclization of β-ketoesters (Scheme 2). In fact, the Pd-catalyzed cyclization of methyl 3-oxo-8-phenoxy-6-octenoate and methyl 3-oxo-8-acetoxy-6-octenoate (which may be considered as a carbon-tethered analogue of the above cyclization precursors) was reported to give a mixture of tetrahydrofuran, vinylcyclopentanone, and cycloheptenone in proportions highly dependent on the reaction conditions.[4]

Scheme 1. Cyclization of Nitrogen-Tethered Substrates[1]

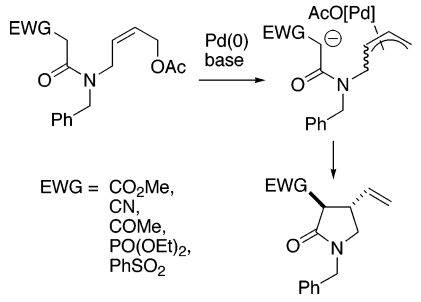

Of the three products, tetrahydrofuran formation is readily reversible, as it can be isolated and subsequently

* Author to whom correspondence should be addressed. E-mail: poli@ccr.jussieu.fr (G.P.); pon@kemi.dtu.dk (P.-O.N.).
§ Technical University of Denmark.
‡ Eli Lilly and Company.
† Université Pierre et Marie Curie.

(1) Giambastiani, G.; Pacini, B.; Porcelloni, M.; Poli, G. *J. Org. Chem.* **1998**, *63*, 804−807. Further studies in the laboratory showed that the old cyclization conditions [$Pd_2(dba)_3$/PPh_3, AcOK cat., THF] could be replaced with those reported in Table 2.

(2) Tsuji, J.; Kobayashi, Y.; Kataoka, H.; Takahashi, T. *Tetrahedron Lett.* **1980**, *21*, 1475−1478.

(3) Koch, G.; Pfaltz, A. *Tetrahedron: Asymmetry* **1996**, *7*, 2213−2216.

(4) In this case, the reversible formation of the tetrahydrofuran derivative **4b** (see Table 2), due to oxygen addition to the η^3-allyl complex, has been clearly demonstrated. See preceding references.

10.1021/om030066d CCC: $25.00
Publication on Web 03/28/2003

Scheme 2. Cyclization of Carbon-Tethered Substrates[2,3]

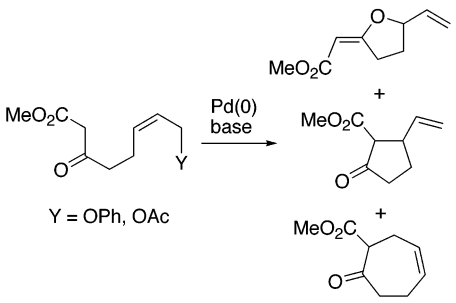

converted to a mixture of cyclopentanone and cycloheptanone under palladium catalysis.[2] In addition, without isolation but longer reaction times, the yield of cyclopentanone increases as tetrahydrofuran decreases.[3] It thus appears that in the β-ketoester series a delicate balance exists between the 5-exo and the 7-endo processes, whereas the nitrogen-tethered series allows exclusively the 5-exo cyclization mode. To obtain further information on the reasons governing the regioselectivity of cyclization, we decided to extend our study to a new precursor incorporating an oxygen-tethering position.

Before presenting our results, some preliminary considerations relative to the prerequisites for cyclization are appropriate. For intramolecular reaction, the initially generated enolate must equilibrate from an *s-trans* to an *s-cis* conformation around the bond between the carbonyl and the tether atom in all cases (CO−X, Scheme 3). The η^3-allyl palladium intermediate normally exists as a mixture of syn and anti isomers in rapid equilibrium compared to the rate of nucleophilic attack (Scheme 3).[5] The syn complex can only react in a 5-exo manner, since endo attack would lead to a highly disfavored *trans*-cycloheptene. The high energy of the syn-7-endo transition state (TS) was verified in one case (vide infra). The anti complex, on the other hand, can allow both 5-exo and 7-endo paths. Thus, three types of transition states (**A**−**C**, Scheme 3) must be considered. Furthermore, enolate/η^3-allyl reaction can take place according to two alternative topologies. The preferred mode is evident from models **A**−**C**, but in one case (X = CH_2), the high-energy transition states **A′**−**C′** were also located. Note that **A′** and **B′** lead to *cis*-**5**, in principle allowing an experimental determination of the preferred enolate face. However, it has been shown that the product undergoes fast epimerization under the reaction conditions, so that only the thermodynamically more stable trans epimer is observed. Thus, the only calculated number that is meaningful to compare to experiments is the total **5**:**6** ratio.

It is important to note that the nitrogen-tethered precursor embeds an amide bond, which in turn forces to planarity the atoms involved in this function (Scheme 3, see bold bonds). Conversely, planarity restriction applies neither to the carbon- nor the oxygen-tethered analogues, and we anticipated that an oxygen-containing substrate would yield both five- and seven-membered-ring products. Thus, we set out to prepare an acyclic oxygen substrate **3** (Scheme 4) and to model the proposed cyclization TS of all three analogues using computational methods.

The Pd-assisted allylic alkylation is one of the most intensely studied organometallic reactions, and the mechanism is well-known.[6] There is no doubt that the selectivity-determining step is the addition of the enolate to an η^3-allyl-Pd intermediate, as depicted in Scheme 3. For the purpose of analyzing selectivities, it is not necessary that the selectivity-determining step also be rate determining, although this is often the case.[6,7] It has previously been demonstrated that a proper transition state for this ionic reaction can be reproduced if, and only if, the effect of the solvent is

Scheme 3. Cyclization of η^3-Allyl-Pd Intermediates, with Newman Projections along the Forming C−C Bonds[a,b]

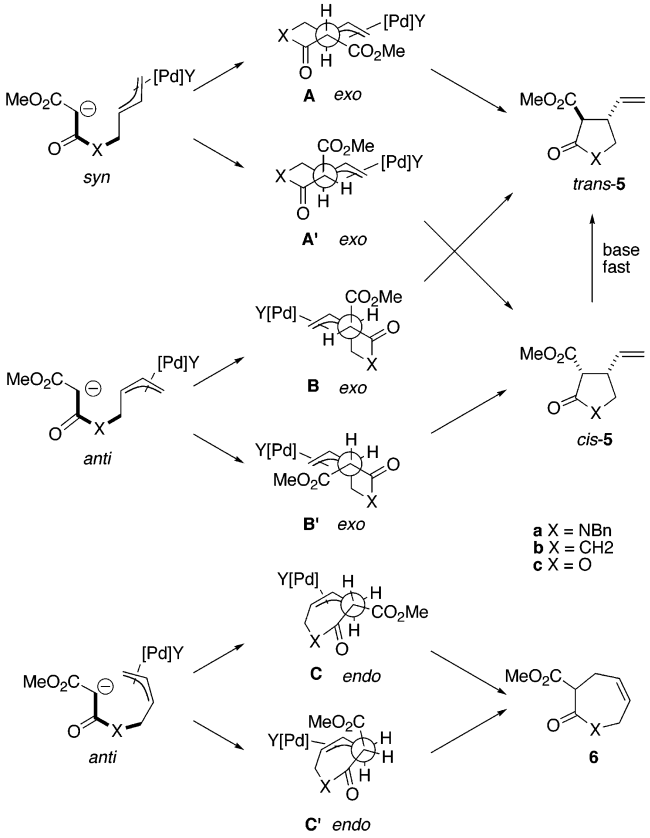

[a] Only relative stereochemistry (*cis*- or *trans*-**5**) is implied. [b] See Table 2 for numbering.

Scheme 4. Preparation and Reactivity of the Oxygen-Tethered Substrates 3a and 3b

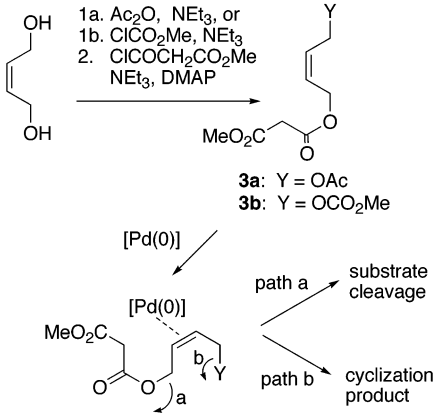

(5) Poli, G.; Scolastico, C. *Chemtracts*: *Org. Chem.* **1999**, *12*, 822−836.

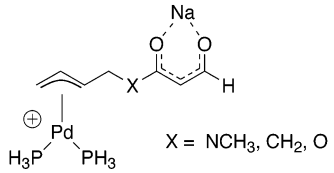

Figure 1. Model system used for DFT calculations.

incorporated.[8] For neutral nucleophiles, a transition state can indeed be located in the gas phase,[9] but even here the structure and activation energy are quite different when the effect of solvent is included.[8] For anionic nucleophiles the gas-phase reaction is barrierless, precluding location of stationary points.[8] The need to account for solvent effects even in the location of stationary points made the calculations demanding, and we therefore decided to work with a small model system. Preliminary force field calculations[10] for the entire complex with the nucleophile constrained to the appropriate approach vector[11] allowed us to identify a suitable model system, where substituents with low influence on the reaction center were capped with hydrogen. The resulting model, depicted in Figure 1, was investigated with density functional theory (DFT). We note that the conformation of the nucleophile is expected to be determined by a chelating coordination. The counterion (Na^+) was therefore included in the calculation. As before,[8] a continuum model was used to capture the effect of the solvent. We chose CH_2Cl_2 as the model solvent because it is one of the most frequently used solvents in the reaction (see Table 2). Although several other solvents have been employed experimentally, the differences between solvent models are marginal relative to the extreme difference between CH_2Cl_2 and the gas phase for the title reaction.[8] The approximations in the calculations (in particular the reduced system size) introduce an uncertainty in the calculated absolute energies, but trends and selectivities, which are obtained from comparing similar structures where systematic errors can cancel, are still expected to be captured accurately at the chosen level of theory.

Table 1. Relative Energies of TS Conformations, by BP86/LACVP*+ (kJ mol^{-1})

entry	tether (X)	TS conform.	product	C···C (Å)[a]	Pd−C···C (deg)[b]	ΔE_{rel} (kJ mol^{-1})[c]
1	NCH_3	A	**5a**	2.44	160	0
2	NCH_3	B	**5a**	2.53	141	13
3	NCH_3	C	**6a**	2.51	126	67
4	CH_2	A	**5b**	2.24	155	2
5	CH_2	A′	**5b**	2.16	152	7
6	CH_2	B	**5b**	2.22	147	7
7	CH_2	B′	**5b**	2.20	163	11
8	CH_2	C	**6b**	2.38	140	0
9	CH_2	C′	**6b**	2.31	139	9
10	O	A	**5c**	2.27	159	0
11	O	B	**5c**	2.33	147	7
12	O	C	**6c**	2.33	139	32

[a] Length of the forming bond. [b] Angle between forming and breaking bonds. [c] Energy relative to the lowest energy TS with the same tether X.

Methods

All calculations were performed in Jaguar v 4.1 or 4.2[12] at the BP86/LACVP*+ level of theory. The LACVP*+ basis set uses the Hay−Wadt small-core ECP basis for Pd,[13] and 6-31+G* for all other atoms. The BP86 functional[14] has recently been recommended for organometallic complexes.[15] The effect of the solvent was simulated by using the PB-SCRF method[16] with parameters appropriate for dichloromethane ($\epsilon = 9.08$, probe radius 2.33237 Å). The model system used in the DFT calculations, with an overall charge of +1, is shown in Figure 1. The sodium ion was chelated to both carbonyl oxygens of the nucleophilic enolate, forming a relatively rigid six-membered ring. Initial transition state structures were located by driving the forming C−C bond with 0.1-Å increments and optimizing all other degrees of freedom, or were generated by hand. All transition states were refined by eigenmode following, converging on gradient only. The quality of the initial Hessian was found to be critical for convergence. The use of a solvent model precluded generation of analytic Hessians. Use of numerical or gas-phase Hessians rarely led to convergence. Instead, best results were generally obtained with the default Hessian refined along selected coordinates (the forming bond and selected angles containing this bond) and additionally along 3−5 low modes of the approximate Hessian. The results are listed in Table 1.

Results and Discussion

Synthesis. The oxygen-tethered cyclization precursors were obtained via monofunctionalization of *Z*-butene-1,4-diol followed by treatment with methyl malonyl chloride (Scheme 4). The first precursor prepared, **3a**, carried the acetate as a leaving group, in analogy to the substrates of the previous studies (steps 1a + 2).

Submission of **3a** to the usual palladium-catalyzed cyclization conditions (NaH, $Pd(OAc)_2$, dppe) gave rise

(6) (a) Trost, B. M.; Verhoeven, T. R. In *Comprehensive Organometallic Chemistry*; Wilkinson, G., Stone, F. G. A., Abel, E. W., Eds.; Pergamon: Oxford, U.K., 1982; Vol. 8, pp 799−938. (b) Godleski, S. A. In *Comprehensive Organic Synthesis*; Trost, B. M., Fleming, I., Semmelhack, M. F., Eds.; Pergamon: Oxford, U.K., 1991; Vol. 4, pp 585−661. (c) Frost, C. G.; Howarth, J.; Williams, J. M. J. *Tetrahedron: Asymmetry* **1992**, *3*, 1089−1122. (d) Reiser, O. *Angew. Chem., Int. Ed. Engl.* **1993**, *32*, 547−549. (e) Harrington, P. J. In *Comprehensive Organometallic Chemistry II*; Abel, E. W., Stone, F. G. A., Wilkinson, G., Hegedus, L. S., Eds.; Pergamon: Oxford, UK, 1995; Vol. 12, p 797. (f) Trost, B. M.; Van Vranken, D. L. *Chem. Rev.* **1996**, *96*, 395−422. (g) Tsuji, J. In *Handbook of Organopalladium Chemistry for Organic Synthesis*; Negishi, E., Ed.; Wiley: New York, 2002; Vol. II, pp 1669−1687.

(7) (a) Åkermark, B.; Hansson, S.; Krakenberger, B.; Vitagliano, A.; Zetterberg, K. *Organometallics* **1984**, *3*, 679−682. (b) Sjögren, M. Selectivity Control in Transition Metal-Catalyzed Nucleophilic Substitution of Allylic Leaving Groups. Ph.D. Thesis, The Royal Institute of Technology, Stockholm, Sweden, 1993.

(8) Hagelin, H.; Åkermark, B.; Norrby, P.-O. *Chem. Eur. J.* **1999**, *5*, 902−909.

(9) (a) Blöchl, P. E.; Togni, A. *Organometallics* **1996**, *15*, 4125−4132. (b) Branchadell, V.; Moreno-Mañas, M.; Pajuelo, F.; Pleixats, R. *Organometallics* **1999**, *18*, 4934−4941. (c) Branchadell, V.; Moreno-Mañas, M.; Pleixats, R. *Organometallics* **2002**, *21*, 2407−2412.

(10) Hagelin, H.; Åkermark, B.; Norrby, P.-O. *Organometallics* **1999**, *18*, 2884−2895. The published force field has been modified to work with enolate nucleophiles. The full force field used here is available from Per-Ola Norrby on request: pon@kemi.dtu.dk.

(11) (a) Oslob, J. D.; Åkermark, B.; Helquist, P.; Norrby, P.-O. *Organometallics* **1997**, *16*, 3015−3021. (b) Farrell, A. Ph.D. Thesis, University College Dublin, 1999.

(12) http://www.schrodinger.com.

(13) Hay, P. J.; Wadt, W. R. *J. Chem. Phys.* **1985**, *82*, 299−310.

(14) (a) Vosko, S. H.; Wilk, L.; Nusair, M. *Can. J. Phys.* **1980**, *58*, 1200−1211. (b) Becke, A. D. *Phys. Rev. A* **1988**, *38*, 3098−3100. (c) Perdew, J. P. *Phys. Rev. B* **1986**, *33*, 8822−8824.

(15) Diedenhofen, M.; Wagener, T.; Frenking, G. In *Computational Organometallic Chemistry*: Cundari, T., Ed.; Marcel Dekker: New York, 2001; pp 69−121.

(16) Marten, B.; Kim, K.; Cortis, C.; Friesner, R. A.; Murphy, R. B.; Ringnalda, M. N.; Sitkoff, D.; Honig, B. *J. Phys. Chem.* **1996**, *100*, 11775−11788.

Table 2. Pd(0)-Catalyzed Intramolecular Allylations of X-Tethered β-Oxo-Esters

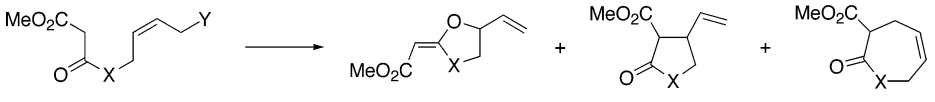

1 X = NCH_2Ph, Y = OAc
2 X = CH_2, Y = OAc, OPh
3 X = O, Y= OAc, OCO_2Me

4 b X = CH_2

5 a X = NCH_2Ph
5 b X = CH_2
5 c X = O

6 b X = CH_2

entry	X	Y	substr.	conditions	solvent	temp (°C)	**4**:**5**:**6**	**5** (%)	ref
1	NBn	OAc	**1a**	NaH, $Pd(OAc)_2$ dppe	DMF	reflux	0:100:0	70[a]	1
2	CH_2	OAc	**2a**	[{$Pd(C_3H_5)Cl$}$_2$] BSA, KOAc, L[c]	DMF	rt	2:66:32	8	3
3	CH_2	OAc	**2a**	[{$Pd(C_3H_5)Cl$}$_2$] BSA, KOAc, L[c]	CH_2Cl_2	rt	55:38:7	22	3
4	CH_2	OPh	**2b**	$Pd(OAc)_2$, PPh_3	MeCN	reflux	0:87:13	59	2
5	CH_2	OPh	**2b**	$Pd(OAc)_2$, $P(OPh)_3$	MeCN	reflux	100:0:0	—[b]	2
6	O	OAc	**3a**	NaH, $Pd(OAc)_2$ dppe	DMF	80		—[d]	—[f]
7	O	OCO_2Me	**3b**	$Pd(OAc)_2$ dppe	DMF	65	0:100:0	25[e]	—[f]

[a] Only trans 3,4-disubstituted lactam. [b] Yield not given. [c] L = Pfaltz's phosphinooxazoline ligand (ref 3). [d] Complex mixture of products. [e] 1:1 mixture of trans and cis 3,4-disubstituted lactones. [f] This work.

to an intractable mixture of products (Table 2, entry 6). We attributed this result to an undesired palladium slippage from the starting olefin η^3-allyl complex (path a), due to the presence of two potentially competing allylic leaving groups. Accordingly, we next prepared by an analogous synthetic protocol (steps 1b + 2) the carbonate precursor **3b**, so as to force generation of the desired η^3-allyl complex (path b) (Scheme 4).[17] Treatment of **3b** with $Pd(OAc)_2$ and dppe in DMF at 65 °C in the absence of base allowed isolation of a diastereoisomeric mixture of the desired γ-lactone **5c**, although in a modest yield (Table 2, entry 7). The already-reported cyclization results for the nitrogen- and carbon-tethered substrates (entries 1−5) are also assembled in Table 2.

Computation

The results from the DFT calculations are listed in Table 1. It can be seen that endo cyclization is disfavored for the nitrogen- and oxygen-tethered systems, but competitive with exo cyclization for the CH_2 substrates **2**, in good agreement with experimental data. Tsuji and Pfaltz noted that the exo vs endo selectivity in the CH_2 case tended to be highly solvent dependent. The results in Table 2 show that the experimental **5**:**6** ratio varies in the range 2−7:1, corresponding to a free energy exo preference of 2−5 kJ mol^{-1} depending on reaction conditions. The calculations indicate a 2 kJ mol^{-1} steric energy preference for the endo path **C**, a very small error considering the approximations used in the model system. For all three tethers, we note that the exo transition states **A** and **B** are considerably less restricted than the endo TS **C**, as seen in the much smaller deviation from the idealized approach vector (≤140° for endo attack, >140° for exo attack, compared to ∼180° for idealized attack[8]). A representative case for the nitrogen tether is depicted in Figure 2. Thus, it is likely that the exo product is favored entropically (i.e., it has a wider range of accessible vectors). A direct calculation of the entropic contribution was beyond our computational resources, but we want to note that the large observed variation in product ratio with reaction conditions also is indicative of a significant entropic contribution.

Looking in more detail at the results for substrate **2b** bearing the carbon tether, we notice that the presumed preference for paths **A**, **B**, and **C** over **A′**, **B′**, and **C′**, respectively, holds, albeit only with a low energy difference between the trajectories (Figure 3). As can be seen in the Newman projections in Scheme 3, the favored paths always put the bulky group of one reaction center gauche to a hydrogen of the other reaction center (paths **A**−**C**), whereas the high energy paths increase the interaction between two bulky groups (paths **A′**−**C′**). The energetic cost is only 4−9 kJ mol^{-1}, making it likely that some cis product is formed initially. However, under basic conditions, any cis product would be expected to epimerize rapidly to the trans product, as shown for the nitrogen-tethered substrate **1**.[1] Thus, the inherent experimental cis preference cannot be estimated from the available data. Since the computational face preference was found to be low and consistent, it was not investigated for the other substrates.

The DFT data indicate that the syn-exo path **A** is faster than the anti-exo path **B** for all substrates (Table 1, Figure 3). It is generally accepted that the syn and anti complexes are present in solution, and in relatively rapid equilibrium,[18] leading to Curtin−Hammett conditions.[19] Hence, formation of **5** mainly through the syn-exo path **A** is expected. However, the anti complex is always the one initially formed from the *Z*-substrates. Thus, the current calculations indicate that if isomerization can be retarded relative to nucleophilic attack, for example by employing phenanthroline ligands,[20] the reaction of *Z*-**2b** could to a higher extent be directed through the anti complex and thus would yield more of the endo product **6b** through path **C**.

For the nitrogen- and oxygen-tethered substrates, **2a** and **2c**, the DFT calculations indicate a high energy penalty for seven-membered-ring formation, by 67 kJ mol^{-1} for **2a** (Figure 2; Table 1, entry 3) and 32 kJ mol^{-1}

(17) The higher reactivity of allylic carbonates with respect to acetates in palladium-catalyzed allylic alkylations is well established: (a) Tsuji, J.; Shimizu, I.; Minami, I.; Ohashi, Y. *Tetrahedron Lett.* **1982**, *23*, 4809−4812. (b) Amatore, C.; Gamez, S.; Jutand, A.; Meyer, G.; Moreno-Mañas, M.; Morral, L.; Pleixats, R. *Chem. Eur. J.* **2000**, *6*, 3372−3376.

(18) Vrieze, K. In *Dynamic Nuclear Magnetic Resonance Spectroscopy*; Jackman, L. M., Cotton, F. A., Eds.; Academic Press: New York, 1975.

(19) Maskill, H. *The Physical Basis of Organic Chemistry*; Oxford University Press: Oxford, UK, 1985.

(20) Sjögren, M.; Hansson, S.; Norrby, P.-O.; Åkermark, B.; Cucciolito, M. E.; Vitagliano, A. *Organometallics* **1992**, *11*, 3954−3964.

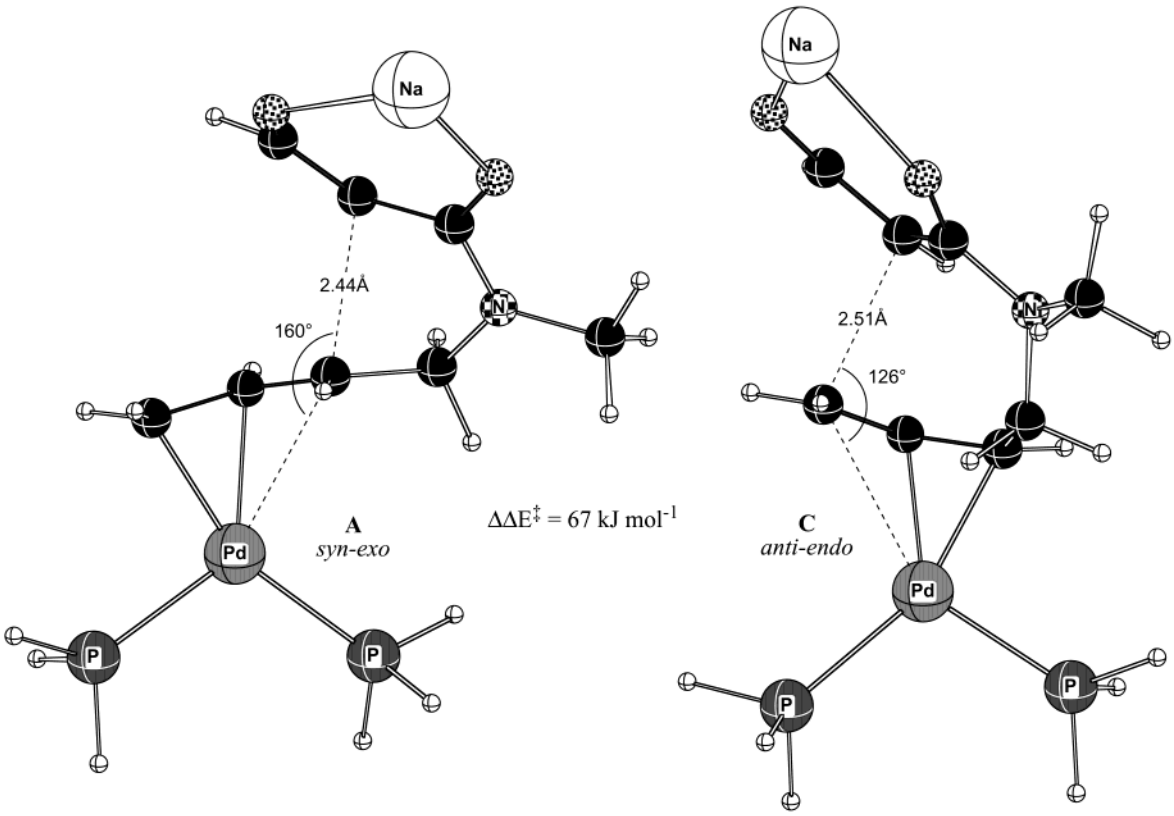

Figure 2. Exo vs endo cyclization for nitrogen-tethered substrate, paths **A** and **C**.

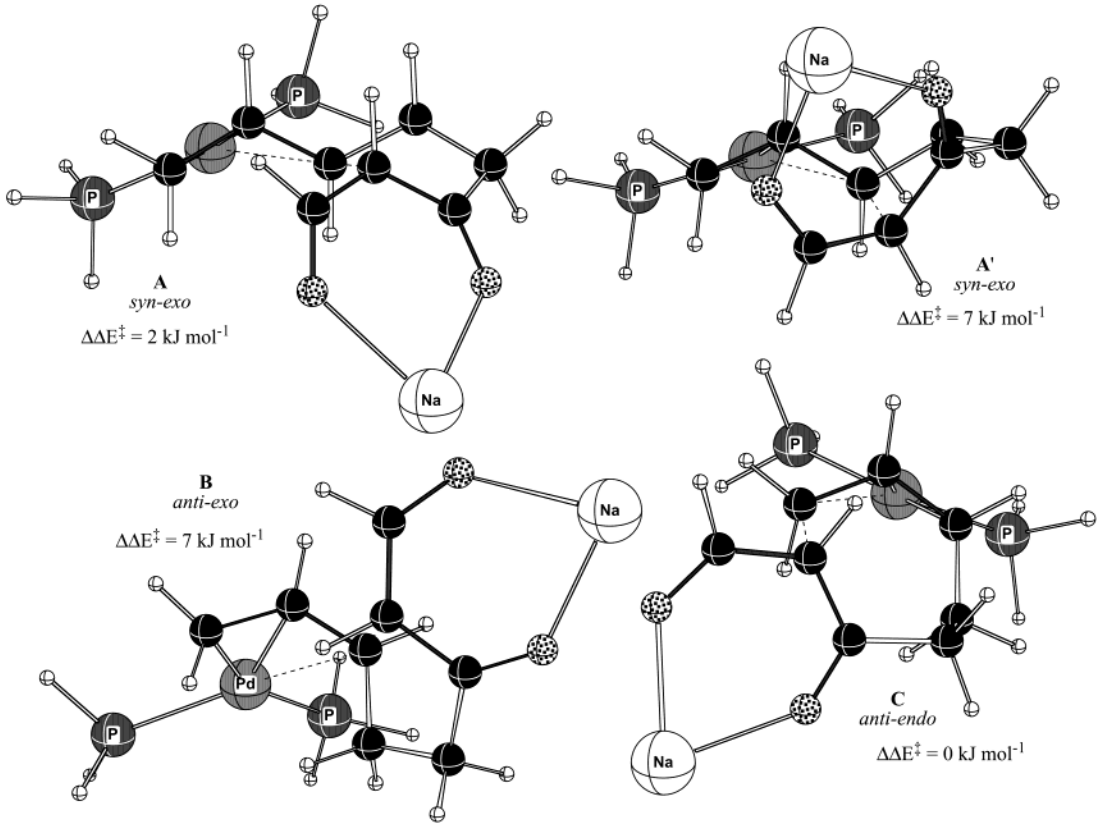

Figure 3. Comparison of paths **A**, **A′**, **B**, and **C**, carbon-tethered substrate.

for **2c** (Figure 4; Table 1, entry 12), in perfect agreement with the exclusive formation of five-membered-ring products **5a** and **5c**, respectively. The structural phenomenon associated with the higher activation barrier for endo cyclization for the nitrogen-containing case is the planarity of the amide center, forcing the substituents about the closure bond into nearly eclipsing positions. Interestingly, the O-*anti-endo* TS is nearly superimposable on the CH_2-*anti-endo* TS, and does not suffer from eclipsing interactions about the closure

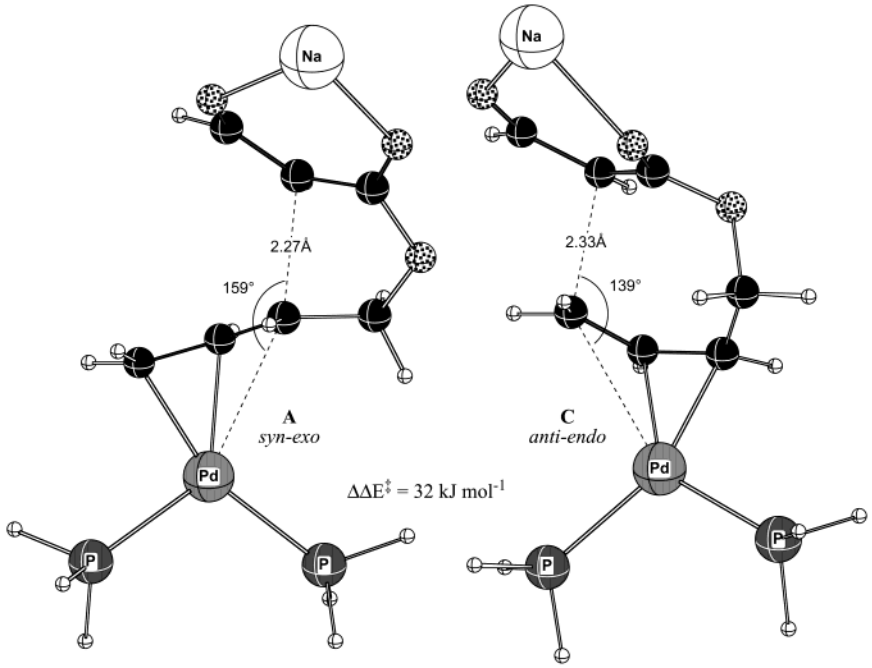

Figure 4. Exo vs endo cyclization for the oxygen-tethered substrate, paths **A** and **C**.

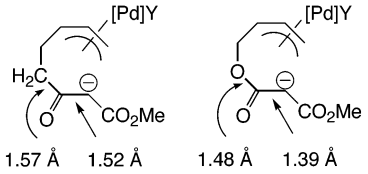

Figure 5. Bond length comparison for endo cyclizations.

bond, and yet endo cyclization is disfavored computationally and is not observed experimentally. However, the bond distances from the carbonyl atom and the two other linked atoms are significantly different (Figure 5), making the transition state substantially more strained in the case of the oxygen tether. Another factor that could have a significant effect upon the relative reactivities is the flexibility of the bond between the oxygen and the allylic carbon atom. The high flexibility here allows the complex to attain a very good approach vector for the syn-exo path **A**, as indicated by an approach angle of 159° (Table 1, entry 10). The same can be seen in the nitrogen-tethered substrate (160°, Table 1, entry 1), whereas the more restricted rotation around the CH_2-CH_2 bond in the carbon-tethered substrate leads to a slightly worse angle of 155° (Table 1, entry 4). Thus, it seems that the high exo preference obtained when employing heteroatom tethers is due both to a selective disfavoring of the anti-endo path **C** (shorter tether, planarity of nitrogen) and a selective favoring of the syn-exo path **A** (more flexible rotation around the CH_2-X bond than around CH_2-CH_2). Of these effects, the amide planarity seems to have the strongest influence.

Conclusions

Computational methods were applied to the Pd-catalyzed intramolecular allylations of resonance-stabilized carbanions deriving from amide, ketone, and ester substrates, with the aim of rationalizing the endo vs exo selectivity in the cyclizations. In addition, ester substrates were prepared and subjected to the Pd-catalyzed cyclization conditions and were found to form lactones via exo attack. DFT calculations with the BP86/LACVP*+ level of theory with a CH_2Cl_2 solvation correction reproduces the experimentally observed trends. The exclusive preference for exo cyclization of the nitrogen-containing starting material appears to result mainly from the preference for near-planarity of the amide N atom. Compared to the carbon-tethered substrates, both heteroatom tethers also disfavor endo cyclization due to the short bonds involved and favor the exo cyclization due to more flexible linking to the allyl moiety. Finally, the exo/endo ratio observed with the carbon tether could be reproduced to within a few kiloJoule per mole.

Experimental Section

General Methods. All reactions were conducted under argon atmosphere. Glassware was flame-dried and then allowed to cool under argon atmosphere before use. All solvents were purified and distilled according to standard methods. Chromatographic purifications were conducted with 40−63 or 15−40 mm silica gel. NMR spectra were recorded on a Brucker ARX 400. IR spectra were recorded on a Perkin-Elmer1420.

(*Z*)-4-(Methyl-malonyl)-but-2-enyl-methyl-carbonate (3b). To a cooled solution of (*Z*)-4-hydroxy-but-2-enyl-methyl-carbonate[21] (6.16 mmol, 900 mg) and pyridine (6.77 mmol, 560 μL) in dichloromethane (15 mL) was added dropwise methyl-3-chloro-3-oxopropionate (6.87 mmol, 725 μL). The mixture was stirred at room temperature for 2 h, before a 1 N HCl solution (10 mL) was added. The aqueous phase was extracted with dichloromethane and the combined organic phases were washed with saturated aqueous $NaHCO_3$ solution (10 mL) and brine (10 mL). Concentration under reduced pressure and flash chromatography (cyclohexane/ethyl acetate 80/20 to 60/40) gave (*Z*)-4-(methyl-malonyl)-but-2-enyl-methyl-carbonate (colorless oil, 1.290 g, 85%). ^{1}H NMR (400 MHz, $CDCl_3$) δ 5.85−5.70 (m, 2H), 4.76 (d, J = 5.6 Hz, 2H), 4.74 (d, J = 5.1 Hz,

(21) Oppolzer, W.; Fürstner, A. *Helv. Chim. Acta* **1993**, *76*, 2329−2337.

2H), 3.79 (s, 3H), 3.75 (s, 3H), 3.40 (s, 2H); ^{13}C NMR (50 MHz, $CDCl_3$) δ 166.51, 165.89, 155.27, 127.76, 127.64, 62.88, 60.58, 54.59, 52.24, 40.85. Anal. Calcd for $C_{10}H_{14}O_7$: C, 48.78; H, 5.73. Found: C, 48.80; H, 5.91. IR (film) cm^{-1}: 2960, 1740, 1440, 1350, 1270, 1150, 1020, 950.

2-Carbomethoxy-3-vinyl-γ-lactone (5c). To a solution of $Pd(OAc)_2$ (13.8 μmol, 3.1 mg) and 1,2-bis(diphenylphosphino)-ethane (27.6 μmol, 11.0 mg) in DMF (0.5 mL) was added a solution of (*Z*)-4-(methyl-malonyl)-but-2-enyl-methyl-carbonate (**3b**, 284 μmol, 70 mg) in DMF (1 mL). The resulting mixture was then stirred at 65 °C for 90 min. A saturated aqueous NH_4Cl solution (20 mL) was added and the aqueous phase was extracted with diethyl ether. The collected organic phases were dried over magnesium sulfate and concentrated under reduced pressure. Flash chromatography (cyclohexane/ethyl acetate 98/2 to 70/30) gave the desired lactone as a 1:1 mixture of diastereoisomers as a colorless oil, 12 mg, 25%). ^{1}H NMR (400 MHz, $CDCl_3$) δ 5.90 (m, 1H), 5.41 (dd, J = 17.3, 7.1 Hz, 1 H), 5.32 (t, J = 10.7 Hz, 1 H), 5.13 (m, 0.5H), 4.90 (dt, J = 9.1, 6.6 Hz, 0.5 H), 3.82 (s, 3H), 3.65 (m, 1H), 2.81 (m, 0.5 H), 2.64 (ddd, J = 9.1, 6.6, 13.1 Hz, 0.5 H), 2.48 (m, 0.5 H), 2.25 (ddd, J = 9.1, 6.6, 13.1 Hz, 0.5 H); ^{13}C NMR (50 MHz, $CDCl_3$) δ 171.3, 168.1, 167.9, 134.8, 134.7, 119.1, 118.2, 79.5, 53.4, 53.1, 47.0, 46.1, 32.4, 32.2; HRMS (M + H^+) calcd for $C_8H_{10}O_4$ 171.0655, found 171.0655.

Acknowledgment. This work was supported by the Comité National de la Recherche Scientifique and by a COST action of the European Community. P.O.N. is grateful to the Danish Natural Sciences Research Council and to the Carlsberg Foundation for funding of computational resources.

Supporting Information Available: Optimized geometries and absolute energies of all stationary points. This material is available free of charge via the Internet at http://pubs.acs.org.

OM030066D